APPLICATION OF A COAL COMBUSTION MODEL IN THE DESIGN OF BLAST PARAMETERS FOR AN IRONMAKING BLAST FURNACE

D. MALDONADO[1], P. ZULLI[1], Y.S. SHEN[2], B.Y. GUO[2] and A.B. YU[2]

[1]BlueScope Steel Research Laboratories, P.O. Box 202, Port Kembla, NSW 2505, AUSTRALIA

[2]Centre for Simulation and Modelling of Particulate Systems, School of Materials Science and Engineering, University of New South Wales, Sydney, NSW 2052, AUSTRALIA

ABSTRACT

With significant economic drivers to reduce consumption of expensive coking coal, Pulverized Coal Injection (PCI) commenced at BlueScope Steel in 2002, at injection rates ranging between 100 and 150 kg-coal/tonne of liquid iron. The key limitation to injection rates is associated with the reduction in packed bed permeability via additional char load into the furnace. The coal is injected via a simple co-axial lance, consisting of an inner pipe (for coal and carrier gas) and an outer annulus (for cooling gas to protect the lance from the high furnace temperatures). The cooling gas can be compressed air, natural gas or pure oxygen. Depending on the choice of cooling gas, the oxygen-to-carbon ratio of the system will change. In this paper, the application of a validated three-dimensional numerical model of the blowpipe/tuyere/raceway is described. The model is used for various plant-specific investigations of blast parameters such as oxygen enrichment, blast temperature and atomic oxygen-to-carbon ratio. The model results show the sensitivity of coal burnout to different operating parameters and confirm that burnouts higher than 80% are difficult to obtain due to the short residence times of the coal.

NOMENCLATURE

A   Arrhenius rate constant
B   Coal burnout
C_D Gas-solid drag coefficient
d_p Particle diameter
e   Char particle void fraction
k_1 Boundary layer diffusion (Gibb equation)
k_2 Surface reaction rate (Gibb equation)
k_3 Internal diffusion rate (Gibb equation)
m_a Ash mass fraction
$m_{a,0}$ Original ash mass fraction
M_C Molecular weight of carbon
Mo_2 Molecular weight of oxygen molecule
Nu   Nusselt number
Pr   Prandtl number
Re   Reynolds number
T_c Activation temperature (K)
T_p Particle temperature (K)
ε_p Particle emissivity
ϕ Molar ratio (Gibb equation)
ρ Density
σ Stefan-Boltzmann constant

INTRODUCTION

Pulverised coal injection was introduced at BlueScope Steel's Port Kembla blast furnaces (BF) in 2002, with aim injection rates in the range of 100-150 kg-coal/tonne of liquid iron. Due to recent changes in supply coal pricing structure, there is a clear economic advantage associated with increasing PCI rates to replace coking coal. Overseas experience, eg from European steelmakers such as Corus IJmuiden and Arcelor Sidmar, suggest that coal injection rates up to and in excess of 200 kg-coal/tonne of liquid iron are sustainable.

Combustion of coal under blast furnace conditions differs from the combustion phenomena experienced in coal fired power stations because of the differences in air temperature, air flow rate, oxygen enrichment and nozzle geometry. Modelling of coal combustion under blast furnace conditions is relatively well advanced (Ishii, 2000).

One of the key factors affecting the maximum PCI rate attainable at the BF is the packed bed permeability – a more permeable bed is more able to cope with the additional char load. In order to minimise char load, the extent of coal combustion (burnout) within the inlet nozzle (tuyere) and raceway must be optimised. This can be achieved through improvements in a) lance design, eg double eccentric lances and/or lance tip shape, b) injection air (blast) parameters, eg oxygen enrichment, cooling gas type, and c) coal type.

Recently, BlueScope Steel Research and University of NSW jointly developed a three-dimensional numerical model to describe the flow and combustion of pulverised coal under BF conditions (Guo et al., 2005). The model was based on the geometry of, and flow conditions used in, BHP Billiton's "third generation" combustion test rig, located at its Newcastle Technology Centre (Mathieson et al., 2003). The original version of the model was developed using the commercial CFD package CFX ver4.4. More recently, a new version of CFX, ver10 (ANSYS CFX, 2006), has been released with an improved coal combustion sub-model within its solver architecture. In addition, the previous version of the model was relatively insensitive to atomic oxygen to carbon (O/C) ratios. This has been addressed by introducing the partial oxidation of char (carbon) to CO, as well as the gasification reactions of char with CO_2 and H_2O. Homogeneous gas phase oxidation reactions of CO and H_2 are also introduced.

MODEL DESCRIPTION

Governing Equations for Gas Phase

The gas phase flow field is described by transport equations of the continuous phase, i.e., three-dimensional, steady-state Reynolds-averaged Navier-Stokes equations, closed by the RNG k-ε turbulence model equations, based on the framework of software package ANSYS-CFX10. Governing equations solved for the gas phase include mass, momentum, turbulence kinetic energy, turbulence dissipation rate, enthalpy, and a number of species mass fractions.

Particle Transport

Pulverised coal particles are treated as a dispersed phase using the Lagrangian method, by which particle behaviours are calculated along the discrete particle trajectories without interaction between particles. The trajectories of the discrete particles are determined by integrating Newton's second law, where the drag force is the main force component. The drag factor C_D is given by Schiller and Naumann (1933) as a function of Reynolds number Re:

$$C_D = 24(1 + 0.15\,\mathrm{Re}^{0.687})/\mathrm{Re} \qquad (1)$$

A number of representative particles are tracked sequentially, one-by-one, in a steady state simulation. The coal particles are treated as non-interacting spheres, each with uniform temperature and composition. Mass conservation is maintained for each particle; however, there is no allowance made for a change in particle volume due to swelling and chemical reaction, ie the internal porosity of the particle increases with mass loss. Full coupling of mass, momentum and energy of particles with the gaseous phase is carried out. Particle dispersion is included in the simulation.

Devolatilisation

Coal combustion consists of a multi-stage process: the devolatilization of a raw coal particle, followed by the gaseous combustion of volatile matter (VM) and the oxidation of the residual char with the oxidant in the gas phase. Devolatilisation is typically modelled as a two-step process (Ubhayakar et al., 1976), in which two reactions with different rate parameters and volatile yields compete to pyrolyse the raw coal, as shown below.

$$\text{Coal} \begin{array}{c} \xrightarrow{k_1} \alpha_1 V_1 + (1-\alpha_1)Ch_1 \\ \xrightarrow{k_2} \alpha_2 V_2 + (1-\alpha_2)Ch_2 \end{array} \qquad (2)$$
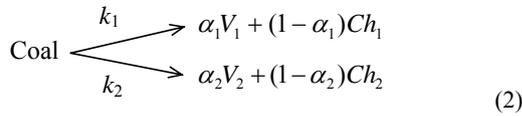
The first reaction dominates at lower temperatures with a lower yield α_1 than the yield α_2 of the second reaction (dominating at temperatures $>\sim 1200$ K). The yield of volatiles at higher temperatures, α_2, depends strongly on temperature and heating rate. A coal dependent Q-factor, or enhancement factor of volatiles yield, is used to adjust the volatile yield, while the low temperature devolatilisation yield, α_1, is based on the proximate VM content (dry ash free basis). Typically Q-factors vary in the range of 1-1.6. The rate constants k_1 and k_2 are particle temperature (T_p) dependent and have an Arrhenius form:

$$k = A\exp(-T_c/T_p) \qquad (3)$$

The default CFX ver 10.0 Arrhenius rate constants and activation temperatures, were used. These are summarised below.

Reaction	A [s^{-1}]	T_c [K]
Low rate (k_1)	3.7×10^5	18000
High rate (k_2)	1.46×10^{13}	30189

Table 1: Coal devolatilisation reaction kinetics

Volatile Matter Composition

The VM consists of C, H and O components, i.e. it is assumed that it has a composition of C_xH_yO, where x and y are a function of ultimate and proximate analyses of the respective coals, as well as a function of the enhancement or Q-factor. In the current study, an interim step is included which assumes the composition of C_xH_yO to consist of H_2, CO and a hydrocarbon, such that:

$$C_xH_yO \rightarrow C_{x-1}H_{y-2z} + z\,H_2 + CO \qquad (4)$$
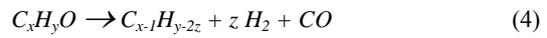
The different yields of hydrogen or hydrocarbon product are dependant on the ultimate and proximate analyses of the coal.

Gas Phase Combustion

The three volatile matter components were assumed to combust with oxygen, as follows:

$$C_\alpha H_\beta + (\alpha+\beta/4)\,O_2 \rightarrow \alpha\,CO_2 + \beta/2\,H_2O \qquad (5)$$

$$H_2 + \tfrac{1}{2}\,O_2 \rightarrow H_2O \qquad (6)$$

$$CO + \tfrac{1}{2}\,O_2 \rightarrow CO_2 \qquad (7)$$

In addition to the above gaseous species, nitrogen, N_2, is also present in the system. The gas compositions are obtained from the solution of transport equations for the mass conservation of each of the components.

Char Oxidation

The char combustion model proposed by Gibb (1985) was used in the current modelling work. Gibb's model takes into account the diffusion of oxygen within the pores of the char particle as well as boundary layer diffusion and reaction kinetics.

In this study two char combustion reactions are considered. They consist of:

$$C + \tfrac{1}{2}\,O_2 \rightarrow CO \qquad (8)$$
$$C + O_2 \rightarrow CO_2 \qquad (9)$$

In addition, CO formed during the partial oxidation of char (Eqn. 8) is assumed to combust to CO_2 (Eqn. 7). The inclusion of the two char oxidation reactions increase the sensitivity of the results to oxygen.

In the Gibb model, the oxidation mechanism of carbon can be characterised by the molar ratio ϕ of carbon atom/oxygen molecules, so that oxides are produced according to the equation:

$$\phi C + O_2 \rightarrow 2(\phi-1)CO + (2-\phi)CO_2 \qquad (10)$$

2
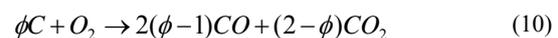
From the above equation it can be seen that as $\phi \rightarrow 1$, the main product consists of CO_2 (Eqn. 9) and as $\phi \rightarrow 2$, the main reaction product consists of CO (Eqn. 8). The molar ratio ϕ is present in the reaction rate developed by Gibb to calculate the rate of decrease in char mass m_c:

$$\frac{dm_C}{dt} = -\frac{3\phi}{1-e} \frac{M_C}{M_{O2}} \frac{\rho_{O_2,\infty}}{\rho_C} (k_1^{-1} + (k_2 + k_3)^{-1})^{-1} \qquad (11)$$

From Eqns. 10-11, it can be seen that the reaction which generates CO as the main product will have a reaction rate which is double the rate of the reaction which generates CO_2 due to the presence of the molar ratio term ϕ in the numerator.

Char Gasification

Two additional heterogeneous gas-char reactions are considered in the current model formulation. These reactions consist of char gasification with CO_2 (solution loss reaction) and H_2O (water gas reaction) as follows:

$$C + CO_2 \rightarrow 2CO \qquad (12)$$

$$C + H_2O \rightarrow CO + H_2 \qquad (13)$$
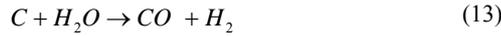
At the high temperatures present in the combustion of coal with enriched oxygen, the above reactions are expected to be limited by external and/or internal diffusion and not by reaction kinetics. As a result, a similar model as the Gibb combustion reaction was adopted to represent the CO_2 and H_2O char gasification reactions. The reaction rate was thus calculated with an equation of the same form as Eqn. 11.

The reaction kinetics were based on char gasification studies conducted by CSIRO at $1100^{\circ}C$ (Hla et al., 2005). The CSIRO gasification studies compared the reactivity of different chars to CO_2 and H_2O; the chars were derived from different Australian coals in a pressurised entrained flow reactor. The equation used in the model to calculate the char oxidation rate was of a *modified* Arrhenius equation of the form:

$$k = A_c T_p \exp(-T_c / T_p) \qquad (14)$$

The values for the Arrhenius parameters are summarised in **Table 2**.

Reaction	A_c [m s^{-1} K^{-1}]	T_c [K]
C- CO_2 gasification	20230	39743
C-H_2O gasification	606.9	32406

Table 2: Char gasification reaction kinetics

Heat Transfer Between Particle and Gas Phase

Both radiation and convection heat transfer are included in the model. The net radiative power absorbed by a particle is calculated by:

$$q_r = \varepsilon_p \pi d_p^2 (I - \sigma T_p^4) \qquad (15)$$

The value of the particle emissivity ε_p is assumed to vary linearly from the raw coal value to the char value as pyrolysis proceeds.

Convective heat transfer due to temperature difference between the fluid and particles is calculated using the Ranz-Marshall correlation (1952):

$$Nu = 2 + 0.6 \, \mathrm{Re}^{0.5} \, \mathrm{Pr}^{0.33} \qquad (16)$$

SIMULATION CONDITIONS

Coal Properties

Five different pulverised coals with wide ranging properties have been used in this study, with volatile matter contents ranging from 5.8 to 39.1% (air dried, ad). The proximate and ultimate analyses of the coals are given in **Tables 3-4**, respectively. It is worthwhile noting that as VM increases, the oxygen content (plus errors) of the coal also increases. This increase is accompanied by a decrease in carbon content, which explains the reduction in gross specific energy.

	Coal 1	Coal 2	Coal 3	Coal 4	Coal 5
Moisture, % (ad)	2.3	0.9	1.2	3.4	5.6
Volatile matter, %(ad)	5.8	12.4	20.0	32.6	39.1
Ash, % (ad)	8.6	8.0	9.7	9.3	2.7
Fixed carbon, % (ad)	83.3	78.7	69.1	54.8	52.6
Gross specific energy, kJ/kg (ad)	33,350	32,975	32,050	31,150	30,470
Q-factor	1.0	1.1	1.1	1.45	1.35

Table 3: Proximate analysis of coals

	Coal 1	Coal 2	Coal 3	Coal 4	Coal 5
C	93.7	91.3	89.1	84.7	79.4
H	3.0	4.0	4.7	5.56	5.6
N	1.1	1.9	1.7	2.1	1.5
S	0.5	0.5	0.37	0.66	0.6
O (by diff)	1.7	2.3	4.1	6.98	12.9

Table 4: Ultimate analysis of coals (%)

The mean particle sizes for the different coal samples varied between 29-54μm. Laser diffraction analyses are summarised in **Fig. 1**.
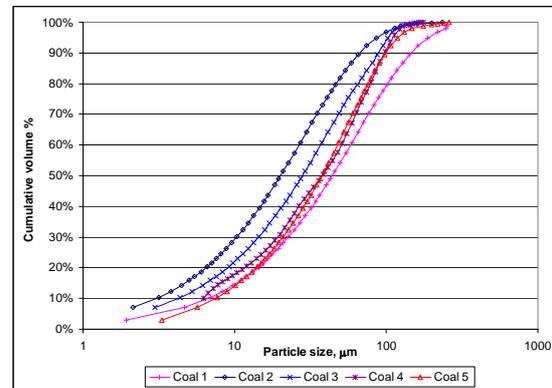

Figure 1: Laser diffraction sizing results for different coals

In the simulations, for each of the coals, 47 particle size classes were sampled in the range of 1 to 250 μm, and a total of 1471 representative particles were tracked.

Geometry and Boundary Conditions

Two different geometries were considered: the BHP-Billiton coal combustion test rig and one of Port Kembla's blast furnace tuyeres. Details of the test rig used to generate the experimental data are described elsewhere (Guo et al., 2005; Mathieson et al., 2003). The main dimensions of the rig and the computational mesh are shown in **Fig. 2**. This is the same mesh used in the study of Guo et al. (2005).
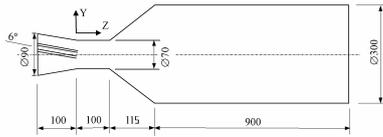
Figure 2: Main dimensions (mm) of the test rig model and outline of computational mesh

The computational model was validated using the above geometry by comparing the predicted coal burnouts with measured values for a variety of coal types tested (Rogers et al., 2006).

Once validated under the test rig conditions, the model was applied to a geometry consisting of a blast furnace blowpipe/tuyere typical of the Port Kembla furnaces, with the appropriate furnace operating parameters used as boundary conditions. This geometry is shown in **Fig. 3**.
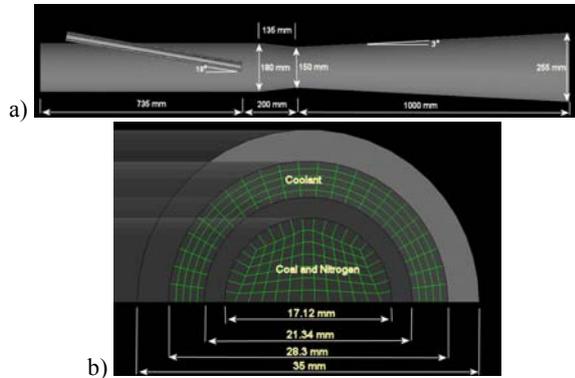

Figure 3: Main dimensions of the BF raceway model

For both geometries, there are three different gas streams entering the domain, namely, conveying gas (nitrogen), cooling gas (either compressed air, oxygen or methane) and hot blast. The flowrates for all three streams are based on experimental and BF operating conditions.

For the test rig simulations, the cases considered were based on the respective coal types for air-cooling. An additional run was undertaken with methane as the coolant for Coal 4, the base case coal (32.5% VM). The boundary conditions for the six cases undertaken for the test rig geometry are shown in **Table 5**. Inlet blast temperature for all cases was 1200°C.

	Total blast flow, $N\text{m}^3/\text{h}$	Blast O_2, %	Coal flow rate, kg/h	Cooling gas flow
Coal 1	301	21.1	27.9	Air, 3.2 $N\text{m}^3/\text{h}$
Coal 2	295	20.8	31.6	Air, 3.2 $N\text{m}^3/\text{h}$
Coal 3	299	20.9	25.2	Air, 3.2 $N\text{m}^3/\text{h}$
Coal 4	306	21.0	22.9	Air, 3.2 $N\text{m}^3/\text{h}$
Coal 5	295	20.8	28.3	Air, 3.2 $N\text{m}^3/\text{h}$
Coal 4	303	20.9	26.9	Methane, 2.8 $N\text{m}^3/\text{h}$

Table 5: Summary of boundary conditions for cases considered in the test rig configuration

The cases for the raceway geometry under blast furnace flow conditions considered the effect of:

- Coal types;
- Cooling gas type (compressed air/oxygen/methane);
- Atomic oxygen-to-carbon ratio;
- Blast temperature; and
- Particle size distribution.

RESULTS

Coal Model Validation

The validation of the coal combustion model formulation was based on a comparison between calculated and measured coal burnouts, with the latter obtained from experimental data after Rogers et al. (2006). The geometry of the test rig is shown in **Fig. 2**. Coal burnout, B, representing the total weight loss of the organic fraction of the coal due to volatile release and char gasification, is calculated using an ash balance:

$$B = (1 - \frac{m_{a,0}}{m_a})/(1 - m_{a,0}) \qquad (17)$$

The measured vs calculated burnouts are summarised in **Table 6** for the respective coals.

	B (measured) (%)	B (calculated) (%)
Coal 1	26.3	54.9
Coal 2	59.8	62.4
Coal 3	63.7	62.9
Coal 4	73.9	72.6
Coal 5	83.2	80.1
Coal 4 (methane cooling)	71.9	68.7

Table 6: Comparison between experimental and calculated burnout

With the exception of Coal 1 (low VM, anthracitic coal), the comparison shows excellent agreement and indicates that the model assumptions and formulation are, within experimental error, very good. The anthracitic coal was a particularly poor burning coal, and possible explanations for its poor performance include low char reactivity, high proportion of coarser particles and poor devolatilisation characteristics.

Blast Furnace Raceway Geometry and Conditions

Based on the same combustion parameters used in the validation of the computational model, simulations were completed for the raceway geometry (**Fig. 3**). Base case boundary conditions consisted of 300,000 Nm^3/h blast flow, 35 t/h coal rate flow (Coal 4), 6000 Nm^3/h oxygen enrichment in blast, 5000 Nm^3/h oxygen cooling flow, 1200°C blast temperature and 45μm mean particle size.

The predicted flow field distributions of various parameters at the symmetry plane for the base case simulation are shown in **Figs. 4-7**.
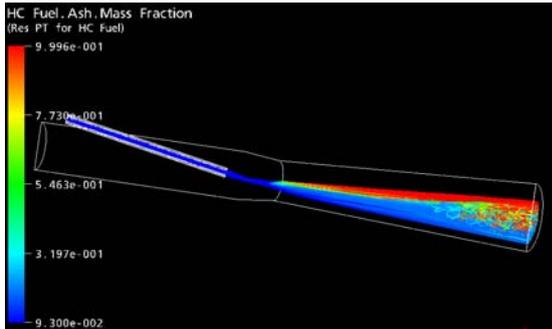
Figure 4: Particle trajectories
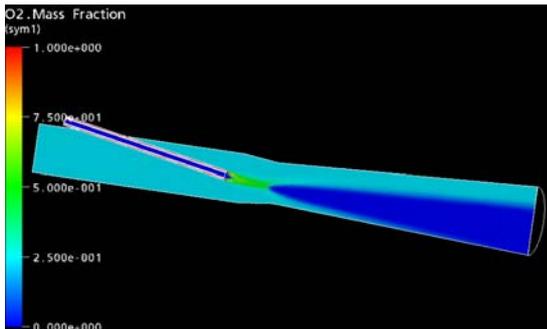
Figure 5: Oxygen mass fraction distribution
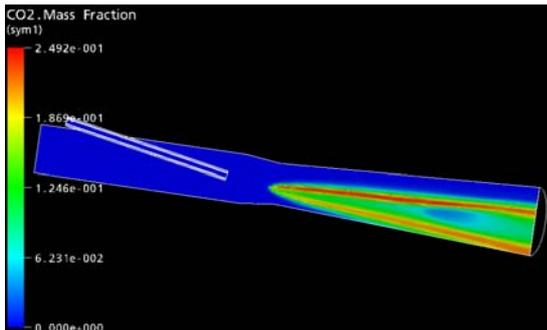
**Figure 6:** CO_2 mass fraction distribution
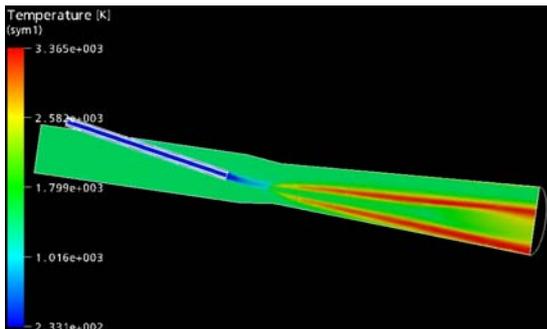
Figure 7: Temperature distribution

The particle trajectories show very little dispersion of the coal (**Fig. 4**). This is consistent with the high blast flow rates, the reduction in cross flow area at the tuyere nose and the adopted shape of the raceway. The coal ash mass fraction is highest near the upper periphery of the plume, which is consistent with the presence of smaller particles in this region and access to oxygen from the gas phase.

Since the coal plume does not disperse significantly, the oxygen mass fraction distribution (**Fig. 5**) shows that the centre of the plume is oxygen-starved and the majority of the char combustion thus takes place around the periphery of the plume. This is where the CO_2 concentration and temperature are highest (**Figs. 6-7**). The distribution of CO_2 shows a reduction in concentration near the end of the raceway. This is where CO_2 and char are in close contact, allowing for the char gasification reactions to take place.

Effect of coal volatile matter

The simulation results for the five different coal types predict a high dependence of coal burnout with volatile matter content (**Fig. 8**). This is because of the much faster reaction kinetics associated with homogeneous phase combustion compared with the char oxidation reactions.
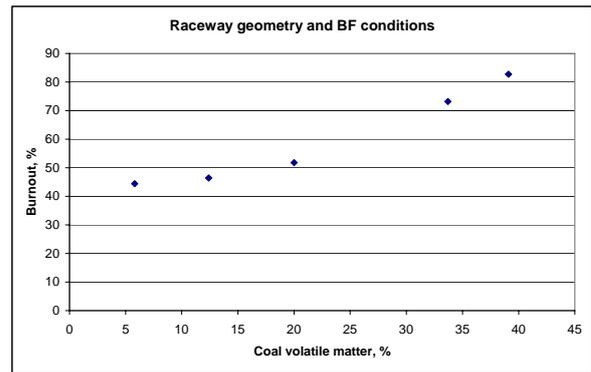

Figure 8: Effect of coal type on burnout for the BF geometry

Effect of cooling gas type

The use of three different types of cooling gas was investigated: natural gas (3000 Nm^3/h), compressed air (5000 Nm^3/h) and oxygen (5000 Nm^3/h). The main blast oxygen enrichment was maintained constant at 6000 Nm^3/h. The burnout results are shown in **Fig. 9**.
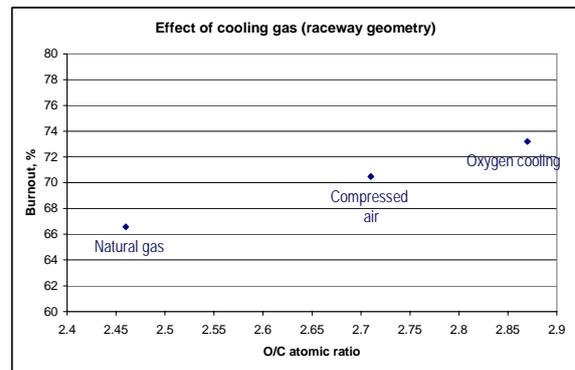

Figure 9: Effect of cooling gas type on coal burnout

A direct relationship exists between the type of cooling gas (denoted by atomic O/C ratio) and coal burnout. This is because in the case of natural gas cooling, the oxygen present in the blast will combust with the natural gas as well as the VM released from the coal. As a result, the amount of oxygen present to carry out the char combustion reaction will be reduced.

Effect of blast temperature

The effect of blast temperature was analysed, viz. 1150°C, 1200°C and 1250°C. The predicted burnout results are shown in **Fig. 10**.
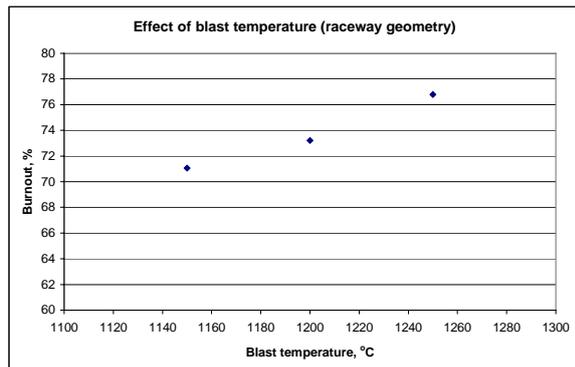

Figure 10: Effect of blast temperature on coal burnout

A direct relationship exists between the blast temperature and the coal burnout. With the higher blast temperatures, coal devolatilisation takes place closer to the lance tip. In addition the peak concentration of volatiles is higher. The resulting volatiles combustion generates additional enthalpy to drive the downstream reactions and in addition, because of the earlier devolatilisation, there is a longer reaction time available in the raceway to consume the char in the slower heterogeneous reactions.

Effect of additional variables

Additional variables which were found to have an effect on coal burnout include the following.

Blast oxygen enrichment –The combination of very high oxygen enrichment and high coal flowrates results in high coal burnouts. Operationally, this is similar to some European blast furnaces. The high coal burnouts are a result of the high oxygen concentration available for volatile matter combustion, the generation of additional enthalpy from the volatile matter combustion and a reduction in blast flow rates, which allows an increase in char residence time in the raceway. The reduction in blast flow rate is associated with the lower nitrogen input into the furnace.

Coal flow rate – Burnout was directly proportional to coal flow rate.

Particle size distribution –The effect of coal particle size distribution is also important. An improvement in coal burnout of 8% (absolute) was predicted when the mean particle size was reduced from 45μm to 29μm as a result of the enhanced coal devolatilisation and char reactivity.

CONCLUSIONS

A numerical model has been developed and validated for the investigation of coal combustion phenomena under blast furnace operating conditions. It was found that:

- Consistent with experimental data, the high Volatile Matter (VM) coals achieve much higher burnouts under simulated raceway conditions;
- A 7% (absolute) improvement in coal burnout is predicted for a lance cooled by compressed oxygen, compared with a lance that is cooled with natural gas;
- Increasing the blast temperature by 50°C to 1250°C resulted in a 4% (absolute) increase in coal burnout;
- The combination of very high oxygen enrichment and high coal flowrates results in high coal burnouts; and
- A reduction in the mean coal particle size from 45μm to 29μm is predicted to increase burnout by 8% (absolute).

ACKNOWLEDGEMENTS

REFERENCES

ISHII, K., (2000), "Advanced Pulverised Coal Injection Technology and Blast Furnace Operation", Elsevier Science Ltd.

GUO, B., ZULLI, P., ROGERS, H., MATHIESON, J. G. and YU, A., (2005), "Three-dimensional Simulation of Flow and Combustion for Pulverised Coal Injection", *ISIJ International*, **45**, 1272-1281.

MATHIESON, J. G., TRUELOVE, J. S. and ROGERS, H., (2003), "Toward an Understanding of Coal Combustion in Blast Furnace Tuyere Injection", *Int. Sym. on Utilisation of Coal and Biomass*, ISUCB-03 Newcastle, Australia.

ANSYS CFX, CFX10.0, (2006), on line document (www.ansys.com/products/cfx.asp)

SCHILLER, L. and NAUMANN, A., (1933), "Uber die Grundlegenden Berechnungen bei der Schwerkraftaufbereitung", *VDI Zeits*, **77**, 318.

UBHAYAKAR, S. J., STICKLER, D. B., von ROSENBERG Jr., C. W. and GANNON, R. E., (1976), "Rapid Devolatilization of Pulverised Coal in Hot Combustion Gases", *16th Symp. (Int.) Combust./The Combustion Institute*, 427.

GIBB, J., (1985), "Combustion of Residual Char Remaining after Devolatilization", Lecture, Mechanical Engineering Dept, Imperial College, London.

HLA, S., HARRIS, D. and ROBERTS, D., (2005), "A Coal Conversion Model for Interpretation and Application of Gasification Reactivity Data", *Proc. Int. Conf. of Coal Sci. and Tech. (ICCS&T)*, Ibaraki, Japan.

RANZ, W. and MARSHALL, W., (1952), "Evaporation from Drops: Part I", *Chemical Engineering Progress*, **48**, 141.

ROGERS, H. (2006), "BlueScope Steel Phase II Blast Furnace PCI Combustion Test Program", Internal BlueScope Steel Report.